Inorg. Chem. **2007**, *46*, 221–230

Supramolecular Assemblies of Trinuclear Triangular Copper(II) Secondary Building Units through Hydrogen Bonds. Generation of Different Metal–Organic Frameworks, Valuable Catalysts for Peroxidative Oxidation of Alkanes

Corrado Di Nicola,[⊥] Yauhen Yu. Karabach,[†] Alexander M. Kirillov,[†] Magda Monari,*[,‡] Luciano Pandolfo,*[,§] Claudio Pettinari,*[,⊥] and Armando J. L. Pombeiro*[,†]

Department of Chemical Sciences, Via S. Agostino 1, University of Camerino, I-62032 Camerino (MC), Italy, Centro de Química Estrutural, Complexo I, Instituto Superior Técnico, Av. Rovisco Pais, 1049-001 Lisbon, Portugal, Department of Chemistry "G. Ciamician", University of Bologna, Via Selmi 2, I-40126 Bologna, Italy, and Department of Chemical Sciences, University of Padova, Via Marzolo 1, I-35131 Padova, Italy

Received August 23, 2006

Formation of the trinuclear triangular copper derivative $[Cu_3(\mu_3\text{-}OH)(\mu\text{-}pz)_3(EtCOO)_2(H_2O)]\cdot H_2O$, **1b** (Hpz = pyrazole), has been simply achieved by addition of Hpz to a water solution of $Cu(EtCOO)_2\cdot H_2O$ and leaving the resulting solution to crystallize at ca. 12 °C. When the reaction and crystallization were carried out at a slightly higher temperature (18–22 °C), the compound $[Cu_3(\mu_3\text{-}OH)(\mu\text{-}pz)_3(EtCOO)_2(H_2O)]$, **1c**, formed. Single-crystal X-ray molecular structure determinations show that both compounds have analogous trinuclear triangular structures, but very different supramolecular assemblies, due mainly, but not only, to the crystallization molecule of H_2O in **1b**. In particular, contrarily to the previously reported, strictly related, $[Cu_3(\mu_3\text{-}OH)(\mu\text{-}pz)_3(EtCOO)_2(EtOH)]$, **1a**, the propionate ions in **1b** and **1c** do not bridge different triangular units, whereas they are involved in intra- and intermolecular H-bonds, generating complex supramolecular 2-D MOFs. Compounds **1a** and **1c** act as remarkably active and selective catalysts or catalyst precursors for liquid biphasic ($MeCN/H_2O$) peroxidative oxidation of cyclohexane and cyclopentane to the corresponding alcohols and ketones.

Introduction

Metal−organic frameworks (MOFs) are receiving great attention not only for their intrinsic structural characteristics but also for their possible applications in gas storage, molecular recognition, catalysis, etc.[1] A great amount of research is currently focused on the preparation and study of suitable secondary building units (SBUs), normally relatively small coordination clusters, that may generate MOFs through supramolecular assembly.[2]

The investigations of polynuclear transition-metal complexes have had a great development in the past decade, also due to the discovery of the fundamental role played by these metal systems in several catalytic biological processes. As an example, copper species are widely found in nature and are present in many enzymes such as di-, tri-, or polynuclear

* To whom correspondence should be addressed. E-mail: magda.monari@unibo.it (M.M.), luciano.pandolfo@unipd.it (L.P.), claudio.pettinari@unicam.it (C.P.), pombeiro@ist.utl.pt. (A.J.L.P.). Phone: +39 051 2099559 (M.M.), +39 049 8275157 (L.P.), +39 0737 402234 (C.P.). +351 218419237 (A.J.L.P.). Fax: +39 051 2099456 (M.M.), +39 049 8275161 (L.P.), +39 0737 637345 (C.P.), +351 218464455 (A.J.L.P.).

[⊥] University of Camerino.

[†] Instituto Superior Técnico.

[‡] University of Bologna.

[§] University of Padova.

(1) (a) Ward, M. D.; McCleverty, J. A.; Jeffery, J. C. *Coord. Chem. Rev.* **2001**, *222*, 251. (b) Eddaudi, M.; Li, H.; Yaghi, O. M. *J. Am. Chem. Soc.* **2000**, *122*, 1391. (c) Moulton, B.; Zaworotko, M. J. *Chem. Rev.* **2001**, *101*, 1629. (d) Janiak, C. *Dalton Trans.* **2003**, 2781. (e) James, S. L. *Chem. Soc. Rev.* **2003**, *32*, 276. (f) Kitagawa, S.; Kitaura, R.; Noro, S-I. *Angew. Chem., Int. Ed.* **2004**, *43*, 2334. (g) Matsuda, R.; Kitaura, R.; Kitagawa, S.; Kubota, Y.; Kobayashi, T. C.; Horike, S.; Takata, M. *J. Am. Chem. Soc.* **2004**, *126*, 14063. (h) Kitagawa, S.; Uemura, K. *Chem. Soc. Rev.* **2005**, *34*, 109. (j) Crowley, J. D.; Bosnich, B. *Eur. J. Inorg. Chem.* **2005**, 2015. (k) Rowsell, J. L. C.; Yaghi, O. M. *Angew. Chem., Int. Ed.* **2005**, *44*, 4670. (l) Kubota, Y.; Takata, M.; Matsuda, R.; Kitaura, R.; Kitagawa, S.; Kato, K.; Sakata, M.; Kobayashi, T. C. *Angew. Chem., Int. Ed.* Engl. **2005**, *44*, 920. (m) Chen, B.; Liang, C.; Yang, J.; Contreras, D. S.; Clancy, Y. L.; Lobkowsky, E. B.; Yaghi, O. M.; Dai. S. *Angew. Chem., Int. Ed.* **2006**, *45*, 1390.

10.1021/ic061595n CCC: $37.00
Published on Web 12/10/2006

systems that selectively catalyze various oxidation reactions.[3] These reactions include, inter alia, those performed by the poorly characterized particulate methane monooxygenase (pMMO) present in methanotrophs, wherein a tri- or multinuclear Cu cluster catalyzes alkane hydroxylation and alkene epoxidation.[3f,j−l] Moreover, trinuclear arrays of copper(II) may be the essential functional units also in a number of multicopper blue oxidases,[4] such as laccase and ascorbate oxidases. In particular, the oxidized active site of the ascorbate oxidases presents a triangular arrangement of copper(II) atoms where the distances between copper ions range from 3.6 to 3.9 Å, and an oxygen (oxo or hydroxo group) bridges the two type-3 copper atoms.[5] Although increasing attention has been paid to the design of Cu complexes with polydentate ligands as models of copper oxidases[3h,k,m,6] the use of multicopper complexes for such reactions still remains a scarcely explored area of research.

Recently, some of us have achieved the easy generation and characterization of copper(II) triethanolamine complexes, adopting di- tri-, tetra-, and polynuclear structures, as well as their catalytic application in alkanes oxidation.[7] Moreover, some of us have reported the easy synthesis of a series of trinuclear triangular Cu(II) clusters, all based on the relatively stable $[Cu_3(\mu_3\text{-}OH)(\mu\text{-}pz)_3]^{2+}$ moiety, through the reaction of copper(II) carboxylates with pyrazole (Hpz).[8] These triangular SBUs spontaneously self-assemble to give different 1-, 2-, or 3-D MOFs, depending on the carboxylate and ancillary ligands.[8b] In these nearly planar triangular $Cu_3(\mu_3\text{-}OH)$ clusters, the tetracoordinated metals show steric accessibility at the axial sites, thus resulting in possible interesting candidates for catalytic processes.

Continuing our studies, here we report the molecular and supramolecular features of three triangular copper(II) propionate SBUs which form different, self-assembled, 3D MOFs. These compounds are remarkably active and selective catalysts or catalyst precursors for the mild peroxidative oxidation of cycloalkanes (viz. cyclohexane and cyclopentane) under mild conditions, into the corresponding alcohols and ketones.

Experimental Section

Materials and Methods. All chemicals were purchased from Aldrich and used without further purification. Copper(II) propionate and compound **1a** were prepared as previously reported.[8b] All reactions and crystallizations were carried out in air. Elemental analyses (C, H, N) were performed with a Fisons Instruments 1108 CHNS-O Elemental Analyzer. A Perkin-Elmer 1100 B Atomic Absorption Spectrometer has been used for quantitative determination of copper. IR spectra were recorded from 4000 to 100 cm^{-1} with a Perkin-Elmer System 2000 FT-IR instrument. The electrical conductances of methanol solutions were measured with a Crison CDTM 522 conductimeter at room temperature. Positive electrospray mass spectra were obtained with a Series 1100 MSI detector HP spectrometer, using MeOH as mobile phase. Solutions for electrospray ionization mass spectrometry (ESI-MS) were prepared using reagent grade methanol, and obtained data (masses and intensities) were compared to those calculated by using the IsoPro isotopic abundance simulator.[9] Peaks containing copper(II) ions are identified as the centers of isotopic clusters. The magnetic susceptibilities were measured at room temperature (20−28 °C) by the Gouy method, with a Sherwood Scientific Magnetic Balance MSB-Auto, using $HgCo(NCS)_4$ as calibrant and corrected for diamagnetism with the appropriate Pascal constants. The magnetic moments (in BM) were calculated from the equation $\mu_{eff} = 2.84(X_m^{corr}T)^{1/2}$. Reflectance solid-state and solution UV−vis spectra were recorded on a Varian Cary 5E spectrophotometer, equipped with a device for reflectance measurements.

Syntheses. $[Cu_3(\mu_3\text{-}OH)(\mu\text{-}pz)_3(EtCOO)_2(H_2O)]\cdot H_2O$, 1b. A solution of 0.306 g of Hpz (4.49 mmol) in 10 mL of water was added to a solution of 1.168 g of $Cu(EtCOO)_2\cdot H_2O$ (4.01 mmol) in 30 mL of water. The resulting deep-blue solution was stirred overnight and then left undisturbed to slowly evaporate in the air,

(2) (a) Yaghi, O. M.; Li, H.; Davis, C.; Richardson, D.; Groy, T. L. *Acc. Chem. Res.* **1998**, *31*, 474. (b) Eddaudi, M.; Moler, D. B.; Li, H.; Chen, B.; Reineke, T. M.; O'Keeffe, M.; Yaghi, O. M. *Acc. Chem. Res.* **2001**, *34*, 319. (c) Eddaudi, M.; Kim, J.; Rosi, N.; Vodak, D.; Wachter, J.; O'Keeffe, M.; Yaghi, O. M. *Science*, **2002**, *295*, 469. (d) Chen, B.; Fronczek, F. R.; Maverick, A. W. *Inorg. Chem.* **2004**, *43*, 8209. (e) Chae, H. K.; Siberio-Pérez, D. Y.; Kim, J.; Eddaudi, M.; Matzger, A. J.; O'Keeffe, M.; Yaghi, O. M. *Nature* **2004**, *427*, 523. (f) Murugavel, R.; Walawalkar, M. G.; Dan, M.; Roesky, H. W.; Rao. C. N. R. *Acc. Chem. Res.* **2004**, *37*, 763. (g) Ockwig, N. W.; Delgado-Friedrichs, O.; O'Keeffe, M.; Yaghi, O. M. *Acc. Chem. Res.* **2005**, *38*, 176. (h) Hofmeier, H.; Shubert, U. S. *Chem. Commun.* **2005**, 2423. (i) Fang, Q.-R.; Zhu, G.-S.; Xue, M.; Sun, J.-Y.; Qiu, S.-L.; Xu, R.-R. *Angew. Chem., Int. Ed.* **2005**, *44*, 3845. (j) Ouellette, W.; Yu, M. H.; O. Connor, C. J.; Hagrman, D.; Zubieta, J. *Angew. Chem., Int. Ed.* **2006**, *45*, 3497; Ding, B.; Yi, L.; Cheng, P.; Liao, D.-Z.; Yan, S.-P. *Inorg. Chem.* **2006**, *45*, 5799.

(3) (a) Solomon, E. I.; Sundaram, U. M.; Machonkin, T. E. *Chem. Rev.* **1996**, *96*, 2563. (b) Kaim, W.; Rall, J. *Angew. Chem., Int. Ed.* **1996**, *35*, 43. (c) Holm, R. H.; Kennepohl, P.; Solomon, E. I. *Chem. Rev.* **1996**, *96*, 2239. (d) Klinman, J. P. *Chem. Rev.* **1996**, *96*, 2541. (e) Cole, A. P.; Root, D. E.; Mukherjiee, P.; Solomon, E. I.; Stack, T. D. P. *Science* **1996**, *273*, 1848. (f) Elliot, S. J.; Zhu, M.; Tso, L.; Nguyen, H.-H. T.; Yip, J. H.-K.; Chan, S. I. *J. Am. Chem. Soc.* **1997**, *119*, 9949. (g) Frausto da Silva, J. J. R.; Williams, R. J. P. *The Biological Chemistry of the Elements*; Oxford University Press: Oxford, 2001. (h) Itoh, S. In *Comprehensive Coordination Chemistry*, 2nd ed.; McCleverty, J. A., Meyer, T. J., Que, L., Tolman, W. B., Eds.; Elsevier: Dordrecht, 2003; Vol. 8, Chapt. 8.15, pp 369−393. (i) Lee D. H. In *Comprehensive Coordination Chemistry*, 2nd ed.; McCleverty, J. A., Meyer, T. J., Que, L., Tolman, W. B., Eds.; Elsevier: Dordrecht, 2003; Vol. 8, Chapt. 8.17, pp 437−457. (j) Ayala, M.; Torres, E. *Appl. Catal. A* **2004**, *272*, 1. (k) Lieberman, R. L.; Rosenzweig, A. C. *Crit. Rev. Biochem. Mol. Biol.* **2004**, *39*, 147. (l) Lieberman, R. L.; Rosenzweig, A. C. *Nature* **2005**, *434*, 177. (m) Yoon, J.; Solomon, E. I. *Inorg. Chem.* **2005**, *44*, 8076.

(4) Huber, R. *Angew. Chem., Int. Ed. Engl.* **1989**, *28*, 848.

(5) Lópèz-Sandoval, H.; Contreras, R.; Escuer, A.; Vicente, R.; Bernès, S.; Nöth, H.; Leigh, G. J.; Barba-Behrens, N. *J. Chem. Soc., Dalton Trans.* **2002**, 2648.

(6) (a) Karlin, K. D.; Zuberbühler, A. D. In *Bioinorganic Catalysis*, 2nd ed.; Reedijk, J., Bouwman, E., Eds.; Dekker, New York, 1999; pp. 469−534. (b) Gamez, P.; Aubel, P. G.; Driessen, W. L.; Reedijk, J. *Chem. Soc. Rev.* **2001**, *30*, 376. (c) Mimmi, M. C.; Gullotti, M.; Santagostini, L.; Battaini, G.; Monzani, E.; Pagliarin, R.; Zoppellaro, G.; Casella, L. *Dalton Trans.* **2004**, 2192. (d) Mirica, L. M; Ottenwaelder, X.; Stack, T. D. P. *Chem. Rev.* **2004**, *104*, 1013. (e) Lewis, E. A.; Tolman, W. B. *Chem. Rev.* **2004**, *104*, 1047.

(7) (a) Kirillov, A. M.; Kopylovich, M. N.; Kirillova, M. V.; Haukka, M.; Guedes da Silva, M. F. C.; Pombeiro, A. J. L. *Angew. Chem., Int. Ed.* **2005**, *44*, 4345. (b) Kirillov, A. M.; Kopylovich, M. N.; Kirillova, M. V.; Karabach, E. Yu.; Haukka, M.; Guedes da Silva, M. F. C.; Pombeiro, A. J. L. *Adv. Synth. Catal.* **2006**, *348*, 159.

(8) (a) Casarin, M.; Corvaja, C.; Di Nicola, C.; Falcomer, D.; Franco, L.; Monari, M.; Pandolfo, L.; Pettinari, C.; Piccinelli, F.; Tagliatesta, P. *Inorg. Chem.* **2004**, *43*, 5865. (b) Casarin, M.; Corvaja, C.; Di Nicola, C.; Falcomer, D.; Franco, L.; Monari, M.; Pandolfo, L.; Pettinari, C.; Piccinelli, F. *Inorg. Chem.* **2005**, *44*, 6265.

(9) Senko, M. W. *IsoPro Isotopic Abundance Simulator*, v. 2.1, National High Magnetic Field Laboratory, Los Alamos National Laboratory: Los Alamos, NM, 1994.

Table 1. Crystal Data and Details of Data Collection for Compounds **1b** and **1c**

	1b	**1c**
formula	$C_{15}H_{24}Cu_3N_6O_7$	$C_{15}H_{22}Cu_3N_6O_6$
fw	591.02	573.01
T, K	293(2)	293(2)
λ, Å	0.71073	0.71073
crystal symmetry	monoclinic	triclinic
space group	*C*2/*c*	$P\bar{1}$
a, Å	28.370(1)	8.0167(9)
b, Å	5.4570(2)	10.259(1)
c, Å	28.123(1)	13.453(2)
α, deg		69.777(3)
β, deg	98.289(2)	88.217(3)
γ, deg		80.496(3)
cell volume, Å^3	4308.3(3)	1023.6(2)
Z	8	2
D_c, mg m^{-3}	1.822	1.859
μ(Mo Kα), mm^{-1}	2.984	3.134
F(000)	2392	578
crystal size, mm	0.10 0.12 0.30	0.07 0.10 0.15
θ limits, deg	1.45−30.07	2.58−24.99
reflections collected	27068 ($\pm h$, $\pm k$, $\pm l$)	8943 ($\pm h$, $\pm k$, $\pm l$)
unique observed reflns [$F_o > 4\sigma(F_o)$]	6317[*R*(int) = 0.0967]	3518[*R*(int) = 0.0513]
GOF on F^2	0.987	1.027
R1 (*F*),[a] wR2 (F^2)[b]	0.0541, 0.1251	0.0753, 0.2038
largest diff peak and hole, e Å^{-3}	0.882 and −1.394	1.700 and −1.006

[a] $R1 = \sum||F_o| - |F_c|/\sum|F_o|$. [b] $wR2 = [\sum w(F_o^2 - F_c^2)^2/\sum w(F_o^2)^2]^{1/2}$ where $w = 1/[\sigma^2(F_o^2) + (aP)^2 + bP]$ where $P = (F_o^2 + 2F_c^2)/3$.

the temperature being maintained in the range 10−14 °C. In a week, light violet thin needles formed, which were separated, washed with two portions of 2 mL of water, and left to dry in air. Yield 0.285 g (36%) based on starting copper. In mother liquors, propionic acid was detected.

1b. Mp: 247 °C dec. Anal. Calcd for $C_{15}H_{24}Cu_3N_6O_7$: C, 30.48; H, 4.09; N, 14.22. Found: C, 30.64; H. 3.92; N, 14.17%. IR (nujol, cm^{-1}): 3671m, 3267br, 1632sh, 1605s, 1566s, 1556s, 1487s, 492m, 465m, 391w, 367s, 326w, 313w, 267br w. μ_{eff} (295 K): 2.202 μ_B. ESI-MS (+) (MeOH) (higher peaks, relative abundance %): 481.9(28) $[Cu_3(OH)(C_3H_3N_2)_3(C_2H_5COO)]$, 531.8(50) $[Cu_3(OH)(C_3H_3N_2)_3(C_2H_5COO)(MeOH)(H_2O)]$; 537.8(47) $[Cu_3(C_3H_3N_2)_3(C_2H_5COO)_2]$; 563.8(80) $[Cu_3(OH)(C_3H_3N_2)_3(C_2H_5COO)(MeOH)_2(H_2O)]$; 606.0(85), $[Cu_3(C_3H_3N_2)_3(C_2H_5COO)_2(H_2O)_2(MeOH)]$; 656.8(45), $[Cu_4(OH)_4(C_3H_3N_2)_2(C_2H_5COO)(H_2O)_3(C_2H_5COOH)]$; 1028.7(32), $[Cu_6(OH)_3(C_3H_3N_2)_7(C_2H_5COO)(H_2O)_3]$; 1064.7(100), $[Cu_6(OH)_3(C_3H_3N_2)_7(C_2H_5COO)(H_2O)_5]$; 1388.6(8), $[Cu_7(OH)_3(C_3H_3N_2)_7(C_2H_5COO)_3(MeOH)(H_2O)_2(C_3H_4N_2)_2]$. Λ_M (MeOH, 1×10^{-4} M) = 14.2 μS/cm.

$[Cu_3(\mu_3\text{-}OH)(\mu\text{-}pz)_3(EtCOO)_2(H_2O)]$, 1c. Compound **1c** was obtained according to the same procedure used for **1b**, but the reaction and the crystallization were performed maintaining the temperature in the range 18−22 °C. A solution of 0.153 g of Hpz (2.25 mmol) in 5 mL of water was added under stirring to a solution of 0.447 g of $Cu(EtCOO)_2 \cdot H_2O$ (1.96 mmol) in 10 mL of water. The resulting solution was left to evaporate and after 5 d, deep-blue blocks were obtained, which were filtered off, washed with water, and dried. Yield 0.305 g (81%) based on starting copper. In mother liquors, propionic acid was detected.

1c. Mp: 242 °C dec. Anal. Calcd for $C_{15}H_{22}Cu_3N_6O_6$: C, 31.44; H, 3.87; N, 14.67. Found: C, 31.58; H 3.84; N, 14.55%. IR (nujol, cm^{-1}): 3300br, 3110w, 1660w, 1568s, 1538s, 1493m, 500w, 490w, 446m, 394w br, 367s, 354w, 325w, 281w, 225m, 216m. μ_{eff} (295 K): 2.318 μ_B. ESI-MS (+) (MeOH) (higher peaks, relative abundance %): 481.9(30), $[Cu_3(OH)(C_3H_3N_2)_3(C_2H_5COO)]$; 531.8-(70), $[Cu_3(OH)(C_3H_3N_2)_3(C_2H_5COO)(MeOH)(H_2O)]$; 537.8(44), $[Cu_3(C_3H_3N_2)_3(C_2H_5COO)_2]$; 564.0(90), $[Cu_3(OH)(C_3H_3N_2)_3(C_2H_5COO)(MeOH)_2(H_2O)]$; 570.0(53), $[Cu_3(C_3H_3N_2)_3(C_2H_5COO)_2(H_2O)_2(MeOH)]$; 606.0(100), $[Cu_3(C_3H_3N_2)_3(C_2H_5COO)_2(H_2O)_2(MeOH)]$; 656.8(40), $[Cu_4(OH)_4(C_3H_3N_2)_2(C_2H_5COO)(H_2O)_3(C_2H_5COOH)]$; 1028.7(10) $[Cu_6(OH)_3(C_3H_3N_2)_7(C_2H_5COO)(H_2O)_3]$; 1064.7(64), $[Cu_6(OH)_3(C_3H_3N_2)_7(C_2H_5COO)(H_2O)_5]$. Λ_M (MeOH, 1×10^{-4} M) = 13.9 μS/cm.

X-ray Crystallography. The X-ray intensity data for **1b** and **1c** were measured on a Bruker AXS SMART 2000 diffractometer, equipped with a CCD detector. Cell dimensions and the orientation matrix were initially determined from a least-squares refinement on reflections measured in three sets of 20 exposures, collected in three different ω regions, and eventually refined against all data. For all crystals, a full sphere of reciprocal space was scanned by 0.3° ω steps, with the detector kept at 5.0 cm from the sample. The software SMART[10] was used for collecting frames of data, indexing reflections, and determination of lattice parameters. The collected frames were then processed for integration by the SAINT program,[10] and an empirical absorption correction was applied using SADABS.[11] The structures were solved by direct methods (SIR 97)[12] and subsequent Fourier syntheses and refined by full-matrix least-squares on F^2 (SHELXTL),[13] using anisotropic thermal parameters for all non-hydrogen atoms. All hydrogen atoms, except the pyrazole and hydroxy hydrogens which were located in the Fourier map and refined isotropically, were added in calculated positions, included in the final stage of refinement with isotropic thermal parameters, $U(H) = 1.2U_{eq}(C)$ [$U(H) = 1.5U_{eq}(C-Me)$], and allowed to ride on their carrier carbons. The methyl carbon [C(15)] of one carboxylate ligand in **1b** was found disordered over two sites and the site occupation factors were refined yielding 0.80 and 0.20, respectively. A crystallization water molecule is also present in **1b** for each trinuclear unit. Crystal data and details of data collection for **1b** and **1c** are reported in Table 1.

Catalytic Activity Studies. The reaction mixtures were prepared as follows: to 0.63−10.0 μmol (typically 10.0 μmol) of catalyst (complex **1c** or **1a**), contained in the reaction flask were added 4.0 mL of MeCN, 0.00−0.30 mmol (typically 0.10 mmol) of HNO_3, 1.00 mmol of cycloalkane (cyclohexane or cyclopentane), and 2.50−10.0 mmol (typically 5.00 mmol) of H_2O_2 (30% in H_2O), in this order. The reaction mixture was stirred for 6 h at room temperature and atmospheric pressure, and then 90 μL of cycloheptanone (as internal standard), 9.0 mL of diethyl ether (to extract the substrate and the products from the reaction mixture), and 1.0 g of PPh_3 (to reduce the organo-hydroperoxides, if formed) were added. The resulting mixture was stirred for 15 min, and then a sample taken from the organic phase was analyzed by GC using a Fisons Instruments GC 8000 series gas chromatograph with a DB WAX fused silica capillary column (P/N 123-7032) and the Jasco-Borwin v.1.50 software. The GC analyses of the aqueous phase showed the presence of only traces (less than 0.05%) of oxidation products. In the experiments with radical traps, the appropriate compounds, e.g., 2,6-di-*tert*-butyl-4-methylphenol (BHT), $CBrCl_3$, or Ph_2NH (2.50 mmol) were also added to the reaction mixture.

(10) Smart & Saint Software Reference Manuals, version 5.051 (Windows NT Version), Bruker Analytical X-ray Instruments Inc.: Madison, WI, 1998.
(11) Sheldrick, G. M. *SADABS, program for empirical absorption correction*, University of Göttingen, Germany, 1996.
(12) Altomare, A.; Cascarano, G.; Giacovazzo, C.; Guagliardi, A.; Moliterni, A. G. G.; Burla, M. C.; Polidori, G.; Camalli, M.; Siliqi, D. *Acta Crystallogr. Sect. A* **1996**, *52*, C79.
(13) Sheldrick, G. M. *SHELXTLplus (Windows NT Version) Structure Determination Package; Version 5.1*., Bruker Analytical X-ray Instruments Inc.: Madison, WI, 1998.

Chart 1

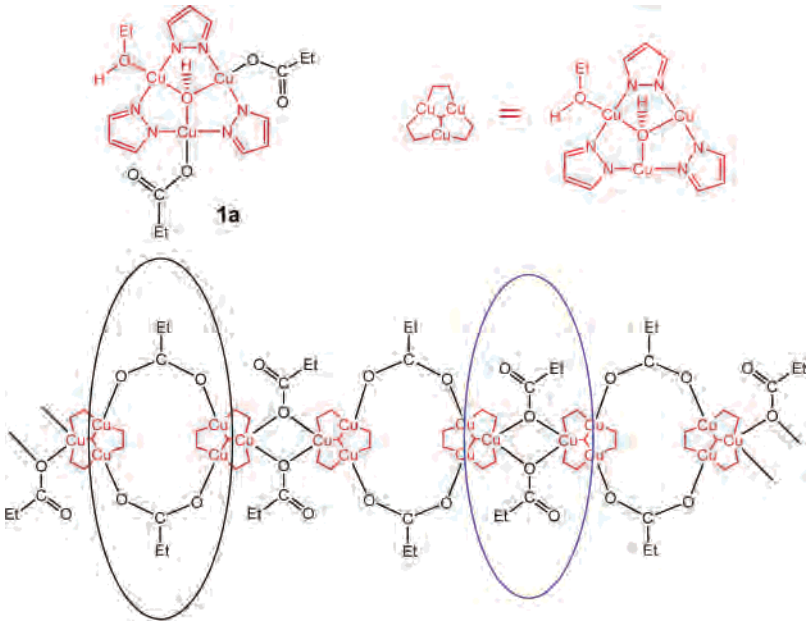

Blank experiments were performed for both cycloalkanes with different amounts of H_2O_2 and other reagents and confirmed that no alkane oxidation products (or only traces, below 0.1%) were obtained in the absence of the metal catalyst.

Results and Discussion

We have recently reported the spontaneous formation of trinuclear triangular Cu(II) clusters whenever $Cu(RCOO)_2$ (R = H, Me, Et, Pr) are reacted with Hpz in water or alcohols. The molecular structures of these clusters, besides the $[Cu_3(\mu_3\text{-OH})(\mu\text{-pz})_3]^{2+}$ moiety, contain two carboxylates and neutral ligands (Hpz and/or reaction/crystallization solvents).[8] Most important, these trinuclear clusters self-assemble giving different 1- or 2-D MOFs depending on the carboxylates and other ligands present in their structures. A description of the effects of these ligands on the supramolecular assemblies has been reported,[8b] but the discussion about some other important factors, as H-bonding, has been explicitly omitted.

Continuing our studies we have performed the reaction between copper(II) propionate and pyrazole in slightly different conditions (ethanol or water as solvent, evaporation carried out at ca. 12 or 18 °C) obtaining three different MOFs. Actually, when the reaction and recrystallization were carried out in ethanol the triangular trinuclear complex $[Cu_3(\mu_3\text{-OH})(\mu\text{-pz})_3(EtCOO)_2(EtOH)]$, **1a**, was obtained, which self-assembled through two different propionate bridges (blue and black ovals) giving rise to the 1-D MOF sketched in Chart 1.[8b]

A deeper analysis of the crystal packing of **1a** also demonstrates, besides the propionate supramolecular interactions, the existence of two kinds of H-bonds. The first one involves the hydrogen of the μ_3-OH bridge of one trinuclear moiety and the uncoordinated propionate oxygen [O(5′)] belonging to the adjacent one (see Figure 1a[14]) [O(1)···O(5′) = 2.705(2) Å, O(1)−H(111)···O(5′) = 166(3)°; symmetry code: (I) $1-x, 1-y, -z$] thus reinforcing the 1-D MOFs. The second kind of H-bond is instead responsible for the interconnection of the 1-D chains to form a 2-D sheet. Each noncoordinated propionate oxygen [O(5)] also interacts with the alcoholic function O(6)H(61) of the coordinated ethanol of a parallel chain, [O(5)···O(6″) = 2.926(2) Å, and O(6″)−H(61″)···O(5) = 164(3)°; symmetry code: (II) $x, y, z-1$].

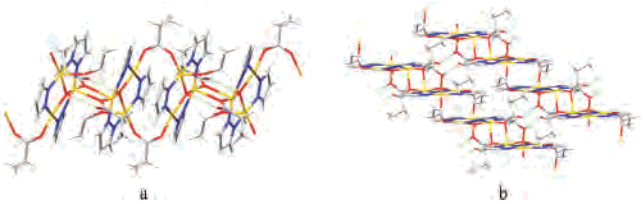

Figure 1. (a) Arbitrary view of **1a** crystal packing showing the 1-D MOF, running along the crystallographic *a*-axis. H-Bonds involving O5 and μ_3-OH are evidenced as green dashed lines. (b) View down an arbitrary direction of the supramolecular assembly of **1a** showing the H-bond interactions (green dashed lines) forming a 2-D sheet by connecting two 1-D MOFs.

If the reaction between copper(II) propionate and Hpz is carried out in water two different compounds, $[Cu_3(\mu_3\text{-OH})(\mu\text{-pz})_3(EtCOO)_2(H_2O)]\cdot H_2O$, **1b**, and $[Cu_3(\mu_3\text{-OH})(\mu\text{-pz})_3(EtCOO)_2(H_2O)]$, **1c**, are obtained, depending on the crystallization temperature. In detail, light-violet needles of **1b** are obtained when the reaction solution is allowed to evaporate at a lower temperature than that used for the preparation of the dark-blue blocks of **1c** (see Experimental Section). Both **1b** and **1c** have trinuclear triangular structures similar to that of **1a**, the coordination of one water molecule instead of ethanol being the most striking difference. Moreover, in **1b**, a further crystallization molecule of water per trinuclear triangular unit is present (Figure 2) in the crystal.

(14) Figure 1 has been obtained by using the CIF file supplied as Supporting Information in ref 8b, to which are also referred the here used atom labels.

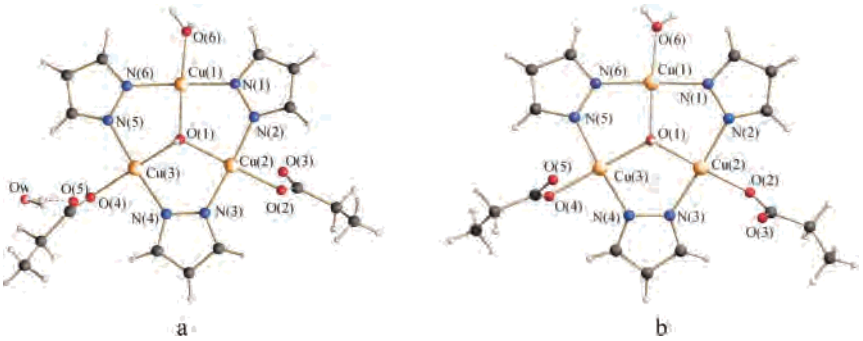

Figure 2. Views of **1b** (a) and **1c** (b), with the atom labeling scheme.

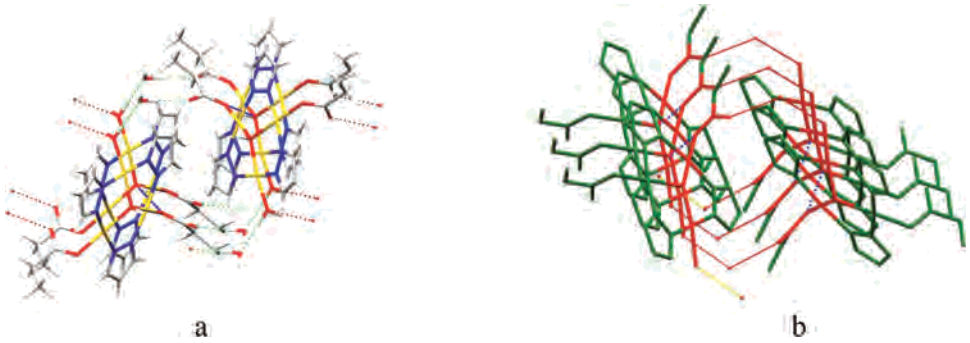

Figure 3. View of the crystal packing of **1b**. (a) H-bond connections (green dashed lines) generating a helical 1-D MOF. (b) Part of a helix formed by three coils (red color) interconnected through O(4)···O(1) H-bonds (blue dashed lines). Hydrogen atoms are omitted for sake of clarity.

Table 2. Selected Bond Lengths (Å) and Angles (deg) for **1b** and **1c**

	1b	**1c**
Cu(1)−O(1)	1.988(3)	1.985(6)
Cu(2)−O(1)	2.010(3)	2.021(6)
Cu(3)−O(1)	1.982(3)	1.976(6)
Cu(1)−N(1)	1.934(3)	1.927(8)
Cu(1)−N(6)	1.943(3)	1.936(7)
Cu(2)−N(2)	1.930(4)	1.952(8)
Cu(2)−N(3)	1.923(4)	1.941(8)
Cu(3)−N(4)	1.936(4)	1.919(8)
Cu(3)−N(5)	1.935(4)	1.926(8)
Cu(2)−O(2)	1.947(3)	1.949(7)
Cu(3)−O(4)	1.974(3)	1.963(6)
Cu(1)−O(6)	1.977(4)	1.969(7)
Cu(1)−O(1)−Cu(2)	113.4(2)	111.4(3)
Cu(1)−O(1)−Cu(3)	115.1(2)	115.5(3)
Cu(2)−O(1)−Cu(3)	115.9(2)	115.9(3)

In spite of the structural similarities of the trinuclear moieties, relevant differences are present in the supramolecular assemblies of **1b** and **1c** with respect to **1a**. As a matter of fact, the crystal packing of both **1b** and **1c** demonstrates that propionate ions do not act as bridges between copper(II) ions of different trinuclear units but are involved into a series of other important intra- and intermolecular H-bonds which generate different, quite complex supramolecular 2-D MOFs.

In **1b**, propionate ions are bound to Cu(2) [Cu(2)−O(2) = 1.947(3) Å] and Cu(3) [Cu(3)−O(4) = 1.974(3) Å] in a monodentate fashion, while a water molecule is the fourth ligand coordinated to Cu(1) [Cu(1)−O(6) = 1.977(4) Å]. Completely similar geometrical features are found in compound **1c**, where Cu(2)−O(2) = 1.949(7), Cu(3)−O(4) = 1.963(6) and Cu(1)−O(6) = 1.969(7) Å. All Cu(II) ions adopt, in both compounds, square planar coordination geometries, a feature rarely observed in other related trinuclear triangular systems.[8,15] Strictly, in compound **1b**, all three Cu ions have a regular square-planar coordination geometry, while in the case of **1c** some deviations from planarity are present, though the geometry is far from the tetrahedral one (see Supporting Information). The most relevant geometrical parameters of **1b** and **1c** are very similar (see Table 2) and in the ranges normally found in the analogous trinuclear triangular derivatives.[8]

The crystal packing of **1b** shows that each trinuclear cluster is connected to other four analogous units through a quite intricate hydrogen bond network that will be described following a series of arbitrary steps. First, the crystallization water molecule is strongly H-bonded to the uncoordinated propionate oxygen atom O(5) [O(5)···O(w)= 2.717(6) Å, O(5)···H(2w)−O(w) = 178°], and the same water molecule is also involved in another strong hydrogen bond with the coordinated water of a second trinuclear unit [O(w)···O(6′) = 2.709(6) Å, O(w)···H(6a′)−O(6′) = 167°]. Such interactions are repeated with a third trinuclear unit and so on, thus generating a 1-D nearly cylindrical helix (Figure 3a) running along a 2-fold screw axis parallel to the crystallographic *b*-axis. Each coil of the helix is formed by two series of 10 atoms {[Cu(1)−O(1)−Cu(3)−O(4)−C(13)−**O(5)**−**H(2w)**−**O(w)**−**H(6a)**−**O(6)**]$_2$} (atoms in bold are the ones involved in hydrogen bonds) disposed to approximately form an ellipse having diameters ranging between ca. 7.71 [(Cu(1)···Cu(1)] and 9.83 [O(w)···O(w)] Å.[16] A series of different hydrogen bonds occurs between the coordinated propionate

(15) In compounds reported in refs 8 Cu(II) ions display mostly the penta- and sometime hexacoordination, reached through supramolecular interactions of carboxylates of nearby trinuclear units or through the coordination of water or alcohols.

(16) Indicated values don't take into account v.d.W radii of involved atoms.

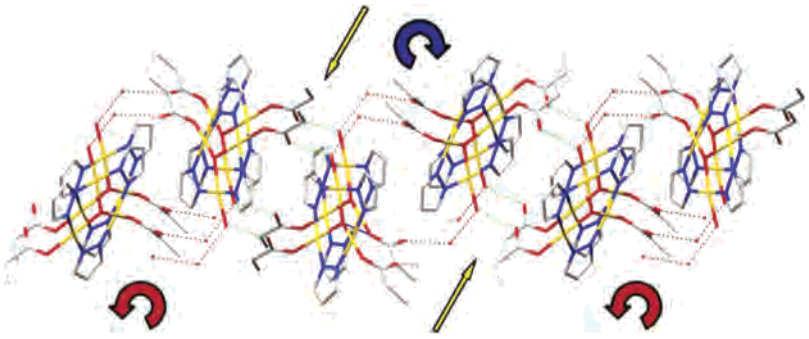

Figure 4. 2-D MOF formed through the O(3‴)···O(6) H-bonds assembly (yellow arrows) of three 1-D helixes (red and blue arrows). Hydrogen atoms are omitted for sake of clarity.

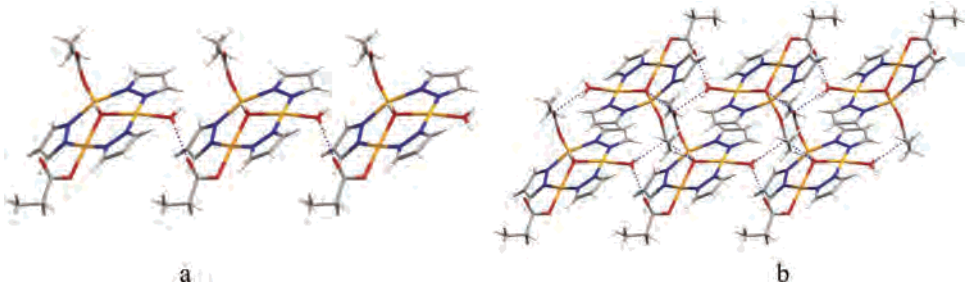

Figure 5. (a) View of **1c** showing the 1-D MOF running along the crystallographic *a*-axis. H-bonds are indicated as blue dashed lines. (b) View of **1c** demonstrating the interactions between two parallel 1-D MOFs. H-bonds are indicated as blue dashed lines. Hydrogen atoms are omitted for sake of clarity.

oxygen [O(4)] of one trinuclear unit and the hydrogen of the μ_3-OH moiety of the nearest, parallel unit [O(4)···O(1″) = 2.691(4) Å, O(4)···H(111″)−O(1″) = 157°; symmetry code: (II) *x*, *y* − 1, *z*]. In Figure 3b, blue dashed lines indicate the O(4)···O(1″) H-bonds, which appear to give a relevant contribution to the helix formation, binding together adjacent coils which result separated by a distance of ca. 5.46 Å.[16]

In Figure 3a are also shown red dashed lines indicating that the coordinated water of each trinuclear cluster strongly interacts, through H(6b), also with the propionate oxygen [O(3‴)] of a further trinuclear unit [O(3‴)···O(6) = 2.600-(5) Å, O(3‴···H(6b)−O(6) = 155°; symmetry code: (III 0.5 − *x*, 1.5 − *y*, 1 − *z*]. Thus, each helix is joined to the other two, generating a 2-D MOF (Figure 4), in which adjacent helixes develop by alternating clockwise (blue arrow) and counterclockwise (red arrows) arrangements, so that each whole sheet is therefore racemic.

These sheets, parallel to the *bc* plane, are stacked each other along the crystallographic *a*-axis, with no apparent bonding interaction among them. Moreover, as confirmed by calculation carried out by using the PLATON routine,[17] in solid **1b** there is no residual solvent accessible area (see Supporting Information).

Dark blue crystals of **1c** are obtained when the reaction solution is let to evaporate at ca. 20 °C[18] (see Experimental Section). While its molecular structure is similar to that of **1b**, the supramolecular assembly generates a 2-D MOF through a H-bond network relatively simpler. In detail, strong H-bonds are formed between the uncoordinated propionate oxygen O(3) and the coordinated water oxygen [O(6′)] of a second trinuclear unit [O(3)···O(6′) = 2.57(1) Å, O(3)··· H(7w′)−O(6′) = 165°; symmetry code: (I) *x* − 1, *y*, *z*], which is connected in the same way with another one and so on, thus generating a 1-D MOF running along the crystallographic *a*-axis (Figure 5a). The same molecule of coordinated water is also connected, through H(6w) with the O(5″) propionate oxygen of a third trinuclear unit [O(6)··· O(5″) = 2.81(1) Å, O(6)−H(6w)···O(5″) = 162°; symmetry code: (II) 2 − *x*, 1 − *y*, −*z*]. The propionate oxygen O(5) is also involved into further H-bond with the μ_3-O(1)H(111) moiety of another trinuclear unit [O(5)···O(1‴) = 2.768(5) Å, O(5)···H(111‴)−O(1‴) 156°; symmetry code: (III) 1 − *x*, 1 − *y*, −*z*]. The overall result is the 2-D MOF[19] shown in Figure 5b.

Compounds **1b** and **1c** are poorly soluble in alcohols and chlorinated solvents and almost insoluble in water, acetone, and acetonitrile. Besides X-ray crystal structure determinations they have been characterized also by elemental analysis, IR spectra, magnetic susceptibility measurements, electronic absorption spectroscopy, and ESI mass spectroscopy. The IR spectra of both compounds show a broad absorption at ca. 3300 cm^{-1}, characteristic of bridging O−H groups derived from both the μ-oxo and coordinated water molecules. The absorptions at ca. 1605, 1566, and 1487 cm^{-1} (**1b**), and 1568, 1538, 1490 cm^{-1} (**1c**), can be assigned to the C═O stretching vibrations of the propionate ions, which

(17) Spek, A. L. *PLATON*, The University of Utrecht, Utrecht, The Netherlands, 1999.

(18) It is noteworthy that if compound **1b** is dissolved in water and the solution left to evaporate at ca. 18 °C, dark blue crystals of **1c** are obtained. It is likely that at ca. 12 °C, one molecule of water remains "frozen" into the crystal lattice, with the help of above described H-bonds.

(19) In the description of the dimensionalities of all reported MOFs here, the trinuclear triangular moieties are considered a 0-D cluster.

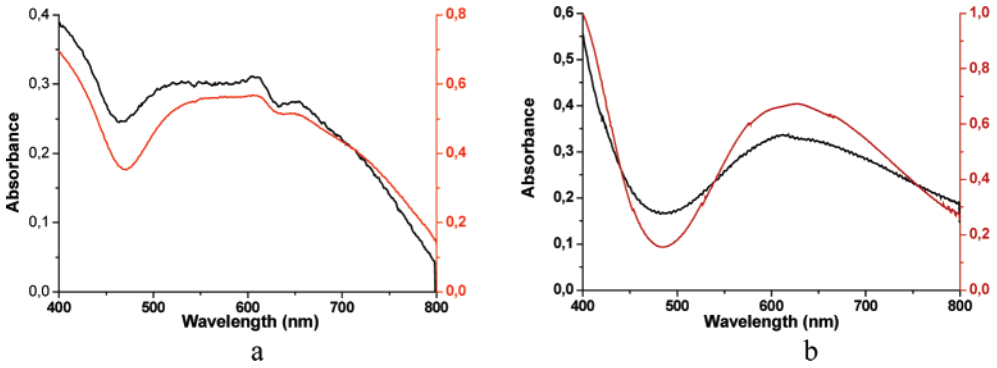

Figure 6. Electronic solid state (a) and MeOH solution (b) spectra of **1b** (black) and **1c** (red).

in these cases act as unidentate unsymmetric ligands[20] and confirm X-ray crystal structure features. Some strong broad bands observed between 507 and 450 cm^{-1} are likely due to Cu−O vibrations.[21]

Room-temperature magnetic susceptibility values of **1b**,**c** range between 2.22 and 2.318 μ_B for each trinuclear unit, quasi-coincident with that previously reported for compound **1a**.[8b] They are lower than those expected for three independent copper(II) ions, indicating some kind of exchange coupling, in accordance to what was previously observed for analogous compounds.[8]

The positive ESI mass spectrum of a methanol/water solution of **1b** shows the most intense signal as a cluster centered at *m*/*z* 1064.7, exactly simulated by $[Cu_6(OH)_3(pz)_7(EtCOO)(H_2O)_5]^+$ and corresponding to two triangular units bridged by hydroxy or pyrazolate groups. Moreover, most of the other relevant signals show patterns typical for ions containing a Cu_3 system, such as the cluster centered at 563.8 (relative intensity 80%), exactly simulated by $[Cu_3(OH)(pz)_3(EtCOO)(MeOH)_2(H_2O)]^+$, formed upon loss of a propionate group from **1b**. As expected, the ESI mass spectrum of **1c** is practically identical to that of **1b** (see Experimental Section).

MeOH solution and solid-state reflectance electronic spectra of **1b**,**c**, in the range 400−800 nm, are reported in Figure 6. Beside two shoulders at about 520 and 710 nm, the reflectance solid-state spectra (Figure 6a) show two evident maxima at ca. 608 and 650 nm. The spectral patterns are only slightly modified in solution (Figure 6b), resulting in the broadening of the two maxima. Both in solid and in solution there are no significant differences among the spectra of **1b** and **1c** and those of **1a** and other parent compounds previously reported.[8]

Peroxidative Oxidation of Cycloalkanes. The trinuclear Cu(II) clusters **1c** and **1a** act as remarkably active and selective catalysts or catalyst precursors for liquid biphasic ($MeCN/H_2O$) peroxidative oxidation (by aqueous H_2O_2 in a slightly acidic medium, at room temperature and atmospheric pressure) of cyclohexane and cyclopentane to the corresponding alcohols and ketones (Chart 2). They lead, in a single batch, to overall yields (based on cycloalkane) up to

Chart 2

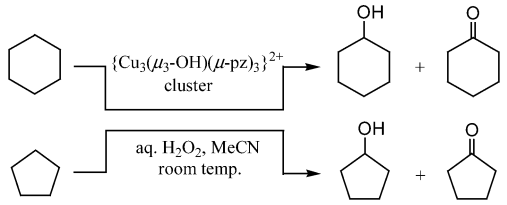

Table 3. Effect of the Acid-to-Catalyst Molar Ratio in the Peroxidative Oxidation of Cyclohexane Catalyzed by **1c**[a]

		yield[b] of products, %		
entry	$n(HNO_3)/n$(catalyst)	cyclohexanol	cyclohexanone	total[c]
1	0.0	0.0	0.0	0.0
2	5.0	6.1	0.3	6.4
3	10	25.1	2.8	27.9
4	20	16.0	1.8	17.8
5	30	13.7	1.6	15.3

[a] Reaction conditions: catalyst (10.0 μmol), C_6H_{12} (1.00 mmol), MeCN (4.0 mL), HNO_3 (0.00−0.30 mmol), H_2O_2 (5.00 mmol). [b] Moles of product/100 mol of cyclohexane. [c] Cyclohexanol + cyclohexanone; overall TON values (moles of products/mol of catalyst) are equal to the total % yield.

32% and turnover numbers (TONs) up to 44 mol of products per mole of catalyst. The influence on the catalytic activity of various parameters such as the relative amounts of nitric acid, hydrogen peroxide, and catalyst, as well as the impact of various radical trapping agents, have been investigated aiming at the optimization of the cycloalkane oxidation processes. The obtained results, shown in Tables 3−6 and Figures 7 and 8, are discussed below.

It was previously described that the peroxidative oxidation of alkanes catalyzed by various V,[22b] Fe,[22a] or Cu[7] catalysts proceeds more efficiently in the presence of nitric acid, since it can play a role toward the activation of catalyst by promoting the unsaturation of the metal center and enhancement of its oxidative properties, the prevention of the decomposition of the peroxide, and the stabilization of intermediate peroxo species.[7] In accord, complex **1c** exhibits no activity for the cyclohexane oxidation in the absence of nitric acid (Table 3, entry 1, Figure 7a), whereas addition of this acid up to 10 equiv relative to **1c** leads to a drastic increase of the total yield of products to 27.9% (entry 3), beyond which the yield drops. The relatively low amount of

(20) Deacon, G. B.; Phillips, R. J. *Coord. Chem. Rev.* **1980**, *33*, 227.
(21) Nakamoto, K. Application in Organometallic Chemistry. *Infrared and Raman Spectra of Inorganic and Coordination Compounds*, 5th ed.; Wiley-Interscience: New York, 1997; p 271.
(22) (a) Kopylovich, M. N.; Kirillov, A. M.; Baev, A. K.; Pombeiro, A. J. L. *J. Mol. Catal. A-Chem.* **2003**, *206*, 163. (b) Reis, P. M.; Silva, J. A. L.; da Silva, J. J. R. F.; Pombeiro, A. J. L. *Chem. Commun.* **2000**, 1845.

Table 4. Effect of the Peroxide-to-Catalyst Molar Ratio and Type of Catalyst in the Peroxidative Oxidation of Cycloalkanes[a]

				yield[b] of products, %		
entry	cycloalkane	catalyst	$n(H_2O_2)/n$(catalyst)	alcohol	ketone	total[c]
1	C_6H_{12}	**1c**	250	2.4	0.3	2.7
2	C_6H_{12}	**1c**	500	25.1	2.8	27.9
3	C_6H_{12}	**1c**	750	23.2	4.4	27.6
4	C_6H_{12}	**1c**	1000	23.6	8.6	32.2
5	C_6H_{12}	**1a**	500	23.0	2.6	25.6
6	C_5H_{10}	**1a**	500	22.6	8.4	31.0
7	C_5H_{10}	**1c**	500	20.2	5.2	25.4

[a] Reaction conditions: catalyst (10.0 μmol), cycloalkane (1.00 mmol), MeCN (4.0 mL), HNO_3 (0.10 mmol), H_2O_2 (2.50−10.00 mmol). [b] Moles of product/100 mol of cycloalkane. [c] Alcohol + ketone; overall TON values (moles of products/mol of catalyst) are equal to the total % yield.

Table 5. Effect of the Amount of Catalyst in the Peroxidative Oxidation of Cyclohexane Catalyzed by **1c** and **1a**[a]

			yield[b] of products, %			
entry	catalyst	catalyst amount, μmol	cyclohexanol	cyclohexanone	total[c]	overall TON[d]
1	−	0.0	0.1	0.0	0.1	−
2	**1c**	0.63	0.0	0.3	0.3	5.1
3	**1c**	1.25	0.9	1.2	2.1	17.0
4	**1c**	2.50	7.8	0.6	8.4	33.6
5	**1c**	5.00	19.5	2.6	22.1	44.2
6	**1c**	10.0	25.1	2.8	27.9	27.9
7	**1a**	0.63	0.1	0.0	0.1	1.1
8	**1a**	1.25	2.6	0.3	2.9	23.1
9	**1a**	2.50	7.9	0.8	8.7	35.0
10	**1a**	5.00	19.0	2.6	21.6	43.3
11	**1a**	10.0	23.0	2.6	25.6	25.6

[a] Reaction conditions: C_6H_{12} (1.00 mmol), MeCN (4.0 mL), $n(HNO_3)/n$(catalyst) = 10, H_2O_2 (5.00 mmol). [b] Moles of product/100 mol of cyclohexane. [c] Cyclohexanol + cyclohexanone. [d] Moles of products/mol of catalyst.

Table 6. Effect of Radical Trapping Agents in the Peroxidative Oxidation of Cyclohexane Catalyzed by **1c**[a]

		yield[b] of products, %			yield drop owing to rad. trap[d] %
entry	radical trap	cyclohexanol	cyclohexanone	total[c]	
1	-	25.1	2.8	27.9	0
2	BHT[e]	5.5	0.0	5.5	80.3
3	$CBrCl_3$	1.0	0.0	1.0	96.4
4	Ph_2NH	5.5	0.0	5.5	80.3

[a] Reaction conditions: radical trap (2.50 mmol), catalyst (10.0 μmol), C_6H_{12} (1.00 mmol), MeCN (4.0 mL), HNO_3 (0.10 mmol), H_2O_2 (5.00 mmol). [b] Moles of product/100 mol of cyclohexane. [c] Cyclohexanol + cyclohexanone. [d] (1 − total yield with radical trap/total yield without radical trap) × 100. [e] BHT = 2,6-di-*tert*-butyl-4-methylphenol.

acid required to reach a maximum of activity of **1c** is in agreement[7] with the low-coordination number of copper and the presence of labile H_2O ligand. A comparable behavior is exhibited by **1a** with the labile EtOH ligand instead of H_2O. On the basis of these observations, further catalytic activity tests were run at the acid-to-catalyst molar ratio of 10.

The amount of hydrogen peroxide also has a pronounced effect and for cyclohexane oxidation catalyzed by **1c**, the increase of the $n(H_2O_2)/n$(catalyst) molar ratio from 250 to 1000 leads to the overall yield enhancement from 2.7 to 32.2%, respectively (Table 4, entries 1−4, Figure 7b). Although this maximum yield is achieved at the highest tested amount of peroxide (entry 4), a quite remarkable total yield of 28% is already reached at the lower peroxide-to-catalyst molar ratio of 500 (entry 2). Compound **1a**, under similar reaction conditions, leads to a slightly lower total yield (25.6%) of cyclohexanol and cyclohexanone (Table 4, entry 5), whereas for the oxidation of cyclopentane, **1a** appears to be more active than **1c**, providing the overall yield of 31.0% (entry 6) vs 25.4% (entry 7) shown by the latter catalyst. Both catalysts **1c** and **1a** exhibit a high selectivity toward the formation of cyclohexanol and cyclopentanol (usually ca. 75−90% of the total amount of products), while the corresponding ketones are obtained in low yields. In addition, a very high overall selectivity of the oxidation reactions (presumably close to 100%) toward the formation of the corresponding alcohols and ketones is observed for both the cyclohexane and cyclopentane oxidations that are catalyzed by **1c** and **1a**. This is supported by GC analyses of the reaction mixtures (both organic and aqueous phases were tested) that show no traces of typical byproducts for peroxidative oxidations of cycloalkanes (e.g., diketones, diols, etc.).

Only traces of cyclohexanol (ca. 0.1%) are detected in the absence of metal catalyst (Table 5, entry 1), and the product yields greatly depend on the amounts of complexes **1c** and **1a** introduced into the reaction mixture. Thus, a yield growth from 0.3 to 27.9% is observed upon increasing the amount of **1c** from 0.63 to 10.0 μmol (Table 5, entries 2−6, Figure 8, curve 1). An enhancement of the overall TON is also detected (Figure 8, curve 2), reaching a maximum of 44 for 5.00 μmol of **1c**, still with preservation of a quite high 22.1% total yield. A similar behavior is also shown by compound **1a** (Table 5, entries 7−11).

The remarkable activity (up to 32% overall yield in a single batch) of compounds **1c** and **1a** is comparable to those of other valuable catalysts for the cyclohexane oxidation based, for example, on multicopper triethanolaminate com-

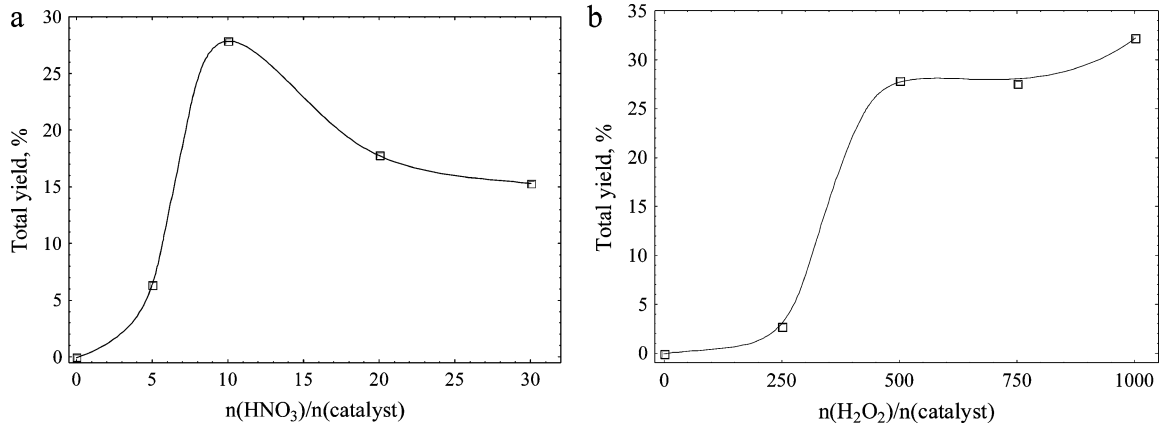

Figure 7. Effect of the acid-to-catalyst (a) and peroxide-to-catalyst (b) molar ratio on the total yield of products in the cyclohexane oxidation catalyzed by **1c**. Reaction conditions are those of Tables 3 and 4.

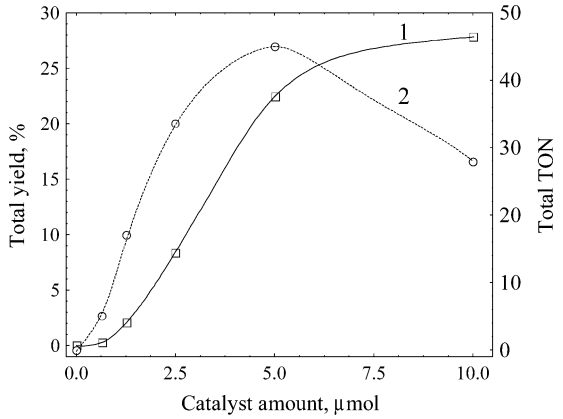

Figure 8. Effect of the catalyst amount on the total yield of products (curve 1) and turnover number of catalyst (curve 2) in the cyclohexane oxidation catalyzed by **1c**. Reaction conditions are those of Table 5.

plexes[7] or hexanuclear iron(III) species[23] and is even higher than those of ca. 18−5% shown by different copper-containing catalytic systems[24] such as Cu salen or acetonitrile complexes, Cu phthalocyanines, or a simple copper salt such as $Cu(NO_3)_2$.[7b] The latter was found to exhibit ca. 5% maximal yield under similar reaction conditions of compounds **1**, thus indicating the relevance of pyrazole and propionate ligands in determining the activity of these complexes. Such ligands can potentially be involved in proton-transfer steps, e.g., among H_2O_2, oxo, and/or peroxo species, as suggested[24b,25] for some V-catalysts that can even require particular N,O additives[25a,b] as cocatalysts. Moreover, the trinuclear Cu complexes **1c** and **1a** appear to exhibit an activity (based on mass) that is higher than that of particulate methane monooxygenase (pMMO), an enzyme with three copper sites at each of its subunits, known to catalyze the hydroxylation of C_1-C_5 alkanes.[3f,j,l] Thus, 143 nmol of cyclopentanol + cyclopentanone and 156 nmol of cyclohexanol + cyclohexanone (averaged over the reaction time) are formed per minute and mg of catalyst **1a** and **1c**, respectively (yields were recalculated from those indicated in Table 4, entries 6, 4), vs 12−17 nmol of ethanol per min·mg of pMMO for the enzymatic hydroxylation of ethane, a particularly favorable substrate for this enzyme.[3f]

Although the oxidation of cyclohexane has been broadly studied[7,25a,26] mainly due to the use of cyclohexanone and cyclohexanol for the production of adipic acid and ϵ-caprolactame in nylon manufacture,[27] only a few data are known regarding the oxidation of cyclopentane,[22a,28] which proceeds usually less efficiently, with the highest reported yield of ca. 19% achieved by using iron(III) hydroxide as catalyst.[22a] In the current work, complex **1a** allows to raise the overall yield of cyclopentanol and cyclopentanone up to 31%, corresponding to one of the most active catalytic systems so far reported for the oxidation of cyclopentane under mild conditions.

The mechanism of the catalysis is still to be established, but a main radical pathway involving both C- and O-centered radicals can be proposed since the oxidation of cyclohexane catalyzed by **1c** is essentially suppressed in the presence of either a carbon-radical trap[29] like bromotrichloromethane or an oxygen-radical trap[29] such as diphenylamine, or 2,6-di-*tert*-butyl-4-methylphenol (BHT) which is known to trap both types of radicals. Thus, the addition of 2.50 mmol of any of these radical trapping agents to the reaction mixture fully suppresses the formation of cyclohexanone, whereas cyclohexanol is then formed in a low yield (1.0−5.5%) that corresponds to a drop of ca. 80−96% (Table 6). The

(23) Trettenhahn, G.; Nagl, M.; Neuwirth, N.; Arion, V. B.; Jary, W.; Pochlauer, P.; Schmid, W. *Angew. Chem., Int. Ed.* **2006**, *45*, 2794.
(24) (a) Velusamy, S.; Punniyamurthy, T. *Tetrahedron Lett.* **2003**, *44*, 8955. (b) Shul'pin, G. B.; Gradinaru, J.; Kozlov, Y. N. *Org. Biomol. Chem.* **2003**, *1*, 3611. (c) Raja, R.; Ratnasamy, P. *Catal. Lett.* **1997**, *48*, 1.
(25) (a) Shul'pin, G. B. *J. Mol. Catal. A-Chem.* **2002**, *189*, 39. (b) Shul'pin, G. B.; Kozlov, Y. N.; Nizova, G. V.; Suss-Fink, G.; Stanislas, S.; Kitaygorodskiy, A.; Kulikova, V. S. *J. Chem. Soc., Perkin Trans. 2.* **2001**, 1351. (c) Reis, P. M.; Silva, J. A. L.; Palavra, A. F.; Frausto da Silva, J. J. R.; Kitamura, T.; Fujiwara, Y.; Pombeiro, A. J. L. *Angew. Chem., Int. Ed.* **2003**, *42*, 821.
(26) (a) Schuchardt, U.; Cardoso, D.; Sercheli, R.; Pereira, R.; da Cruz, R. S.; Guerreiro, M. C.; Mandelli, D.; Spinace, E. V.; Pires, E. L. *J. Appl. Cat. A-Gen.* **2001**, *211*, 1. (b) Shilov, A. E.; Shul'pin, G. B. *Activation and Catalytic Reactions of Saturated Hydrocarbons in the Presence of Metal Complexes*; Kluwer Academic Publishers: Dordrecht, The Netherlands, 2000.
(27) *Ullmann's Encyclopedia of Industrial Chemistry*, 6th ed.; Wiley-VCH: Weinheim, 2002.
(28) (a) Teramura, K.; Tanaka, T.; Hosokawa, T.; Ohuchi, T.; Kani, M.; Funabiki, T. *Catal. Today* **2004**, *96*, 205. (b) LeCloux, D. D.; Barrios, A. M.; Lippard, S. J. *Bioorg. Med. Chem.* **1999**, *7*, 763. (c) Yamanaka, I.; Nakagaki, K.; Akimoto, T.; Otsuka, K. *J. Chem. Soc., Perkin Trans. 2* **1996**, 2511.
(29) Slaughter, L. M.; Collman, J. P.; Eberspacher, T. A.; Brauman, J. I. *Inorg. Chem.* **2004**, *43*, 5198.

involvement of radicals is also supported by the detection in the final reaction mixtures, following a method of Shul'pin et al.,[25a,26b] of the corresponding organo-hydroperoxides ROOH (R = C_6H_{11}, C_5H_9) which are usually formed in radical type oxidations. The formation of intermediate copper-peroxo species can also occur upon reaction of the $[Cu_3(\mu_3\text{-}OH)(\mu\text{-}pz)_3]^{2+}$ core with hydrogen peroxide. In this respect, it is worthwhile to mention that a great part of the still rare structurally characterized examples[30] of peroxo Cu compounds is stabilized by pyrazole or derived ligands.[31]

Conclusions

H-bonds are recognized as one of the most relevant noncovalent interactions in supramolecular chemistry and crystal design.[32] Water is very often involved into such interactions and is present as coordinated or crystallization molecule(s) in a large number of MOFs.

In this work we have reported that very subtle modifications in the synthetic and/or crystallization conditions, actually the use of ethanol or water as solvent and slightly different crystallization temperatures, generate strongly different MOFs. Particularly, in the case of **1b** and **1c** the propionate ions are involved in strong H-bonds with coordinated (**1c**) and both coordinated and crystallization water (**1b**); thus, they cannot bridge Cu(II) ions as observed in **1a**.[8b] Moreover, in both compounds, coordinated water forms H-bonds with the uncoordinated oxygen [O(3)] of one propionate belonging to another trinuclear unit, according to very similar geometrical parameters. Thus, the differences between the two MOFs are due to the fact that in **1b**, coordinated water also interacts with the crystallization water that is, in turn, connected with the uncoordinated oxygen [O(5)] of the second propionate belonging to a third trinuclear unit, while in **1c** the second interaction of coordinated water occurs directly with O(5) of a third trinuclear unit. In other words, the "interference" of the crystallization water molecule in **1b** pushes away the third trinuclear unit [O(6′)⋯O(5) = 4.619 Å], and this generates a very different MOF with respect to **1c**. In conclusion, in our specific cases the presence of water forbids, or at least makes more difficult, other fragments (the propionate ions) from having noncovalent interactions different from H-bonds.

Moreover, it is quite interesting that both **1a** and **1c** show similar but not identical catalytic properties. As a matter of fact, **1a** results in one of the most efficient catalysts (or catalyst precursors) reported until now for the mild peroxidative oxidation of cyclopentane, while **1c** is more active toward the oxidation of cyclohexane. Even though we have no proof, it seems likely that the supramolecular structure, or at least the coordination of EtOH, is maintained when **1a** is dissolved in water or in the liquid aqueous biphasic medium which is employed in the oxidation experiments. Further studies are currently in progress on these and other related polynuclear Cu(II) complexes, to illustrate their supramolecular arrangements and to test their catalytic properties.

Acknowledgment. The Universities of Bologna, Camerino, and Padova are gratefully acknowledged. This work has been partially supported by the Foundation for Science and Technology (FCT) and its POCTI and POCI 2010 programmes (FEDER funded) as well as by the Human Resources and Mobility Marie Curie Research Training Network (AQUACHEM project, CMTN-CT-2003-503864).

Supporting Information Available: X-ray crystallographic files in CIF format for the structure determinations of **1b** and **1c**, figures showing the square planar coordination around all Cu(II) ions of **1b** and **1c**, figures showing deviations from planarity of **1b** and **1c**, crystal packing of **1b** and **1c**. This material is available free of charge via the Internet at http://pubs.acs.org.

IC061595N

(30) Allen, F. H. *Acta Crystallogr.* **2002**, *B58*, 380.
(31) (a) Meyer, F.; Pritzkow, H. *Angew. Chem., Int. Ed.* **2000**, *39*, 2112. (b) Hu, Z.; George, G. N.; Gorun, S. M. *Inorg. Chem.* **2001**, *40*, 4812. (c) Fujisawa, K.; Tanaka, M.; Moro-oka, Y.; Kitajima, N. *J. Am. Chem. Soc.* **1994**, *116*, 12079.
(32) (a) Desiraju, G. R. *Comprehensive Supramolecular Chemistry*; Pergamon Press: Oxford, 1996; Vol. 6. (b) Jeffrey, G. A. *J. Mol. Struct.* **1999**, *486*, 293; (c) Odriozola, L.; Kyritsakas, N.; Lehn, J.-M. *Chem. Commun.* **2004**, 62.